Error estimation and adaptivity in elastoplasticity

L. Gallimard, Pierre Ladevèze, Jean-Pierre Pelle

ERROR ESTIMATION AND ADAPTIVITY IN ELASTOPLASTICITY

L. GALLIMARD, P. LADEVÈZE AND J. P. PELLE

Laboratoire de Mécanique et Technologie, ENS de Cachan/CNRS/Université P. et M. Curie, 61 Avenue du Président Wilson, 94235 Cachan Cedex, France

SUMMARY

In this paper, a method is developed to control the parameters of a finite element computation for time-dependent material models. This method allows the user to obtain a prescribed accuracy with a computational cost as low as possible. To evaluate discretization errors, we use a global error measure in constitutive relation based on Drucker's inequality. This error includes, over the studied time interval, the error of the finite element model and the error of the algorithm being used. In order to master the size of the elements of the mesh and the length of the time increments, an error estimator, which permits estimating the errors due to the time discretization, is proposed. These tools are used to elaborate two procedures of adaptivity. Various examples for monotonous or non-monotonous loadings, for 2-D or axisymmetric problems, show the reliability of these procedures.

KEY WORDS: *a posteriori* error; finite element; plasticity, adaptativity

INTRODUCTION

Today, industry requires the resolution of highly complex problems: 3-D problems, non-linear material behaviour, contacts, large deformations, etc. For these problems, the economic aspects are very important: computation time, time necessary to prepare the computation (especially the meshing of complex structures), amount of data to store, etc. To perform such analyses, it is imperative, even within the framework of using more and more efficient computers, to master the parameters of the computation (size of the elements, type of elements, time increment length) in order to minimize the computional costs while obtaining a prescribed accuracy.

The aim of this article is to study these questions for the computation of structures with a non-linear material behaviour (elastoplasticity for instance), under the assumption of small displacements and for quasi-static loading.

Numerous studies have dealt with the problem of adaptive control for linear problems;[1-8] in comparison, few studies deal with the non-linear problems, especially with rate-dependent model problems.[4,8-19]

In elastoplasticity, the quality of the finite element solution at the instant t depends not only on the quality of the mesh, but also on the quality of the time discretization used since the beginning of the loading. Mastering such an analysis is thus clearly more complex than for linear static problems. In particular, the approach which consists of applying directly the procedures used in statics, at certain time steps, is insufficient to estimate the quality of such a computation. To master a non-linear computation, it is therefore necessary to build error measures that allow, over the whole time interval $[0, T]$, to take into account all the errors of discretization: errors due to

the mesh, errors due to the incremental method (including the errors introduced by the use of Newton's method on each time increment). An error in constitutive relation ε, having these properties and a strong mechanical meaning, has been proposed by Ladevèze.[20] This error measure is based both on Drucker's inequality,[21] which is satisfied by most of the elastoplastic and viscoplastic material models, and on techniques to construct admissible fields. An initial implementation for plane stress problems and for 3-node triangular elements as well as procedures allowing to master the meshes, have been proposed by Coffignal *et al.*[4] The definition of this error measure and its main properties are recalled in the first part of this work.

In the second part, we present techniques which allow building, by post-processing the finite element solution, a stress field which verifies at each instant t the equilibrium equations. An important point is that these techniques are independent of the algorithm used to solve the non-linear problem.

The error measure in constitutive relation ε takes into account simultaneously the errors due to the space discretization and the errors due to the incremental method. To control the parameters of the computation (size of the elements and size of the time increments), it is necessary to separate the contribution due to the incremental method from the contribution due to the mesh. To solve this difficulty, we propose a time error indicator which permits, for a given space discretization, estimating the part of the error due to the time approximations.

Using these two error indicators, a rather simple procedure of adaptivity is initially proposed. Various examples of monotonous and non-monotonous loading show the possibilities of this procedure; for these examples, we use the Prandtl–Reuss model. Then, a more elaborate procedure is given. This procedure enables us to adapt simultaneously the mesh and the time discretization.

ERROR IN CONSTITUTIVE RELATION

For purposes of simplicity, let us consider the problem of the analysis of a structure in 2-D elastoplasticity (plane stress or plane strain). Yet, all the concepts can be extended without any difficulty to axisymmetric or 3-D computations.

Notation

Let $[0, T]$ be the time interval. Let us suppose that the structure is a domain Ω. On a part $\partial_1\Omega$ of the boundary $\partial\Omega$, we suppose that the imposed displacement field is

$$U(t, M) = U_d(t, M)$$

On the complementary part

$$\partial_2\Omega = \partial\Omega - \partial_1\Omega$$

a density of forces $F_d(t, M)$ is imposed. Moreover, Ω is submitted to a density of body forces $f_d(t, M)$.

In elastoplasticity, the value of the stress at t is a function of the history of the strain at the instant t, that may be translated, at each point current M of the structure Ω, by the relation

$$\sigma(t, M) = \mathbf{A}[\varepsilon(t', M), t' \leqslant t] \tag{1}$$

where $\mathbf{A}$ is an operator characteristic of the material and ε is the strain field.

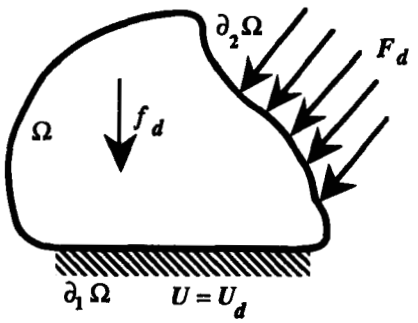

Figure 1. Notation

Reference problem

The elastoplastic problem can be formulated in the following manner: *Find a displacement field* U *and a stress field* σ *defined on* $[0, T] \times \Omega$ *such that*:

(a) U *satisfies the kinematic constraints*:

$$\forall t \in [0, T] \quad U(t, M) = U_d(t, M) \quad \text{on } \partial_1\Omega \tag{2a}$$

(b) σ *satisfies the equilibrium equations*: $\forall t \in [0, T]$

$$\begin{gathered} \forall U^* \text{ such that } U^* = 0 \text{ on } \partial_1\Omega \\ \int_\Omega \sigma^{\mathrm{T}} \varepsilon(U^*)\, \mathrm{d}\Omega = \int_\Omega f_d^{\mathrm{T}} U^*\, \mathrm{d}\Omega + \int_{\partial_2\Omega} F_d^{\mathrm{T}} U^*\, \mathrm{d}S \end{gathered} \tag{2b}$$

(c) σ *and the strain* $\varepsilon(U)$ *satisfy the constitutive relation*:

$$\forall t \in [0, T] \quad \sigma(t, M) = \mathbf{A}[\varepsilon(U)(t', M), t' \leqslant t] \quad \text{in } \Omega \tag{2c}$$

(d) *at* $t = 0$, *the structure is in a natural state*:

$$\forall M \in \Omega \quad U(0, M) = 0, \quad \sigma(0, M) = 0 \tag{2d}$$

Discretization

The problem (2) is solved in an approximate manner by using the incremental method and a finite element discretization. The time interval $[0, T]$ is subdivided into increments:

$$0 < t_1 < t_2 < \cdots < t_i < \cdots < T$$

With the history of the displacements and of the stresses being known up until t_i, the problem is then to compute this history on the increment $[t_i, t_{i+1}]$. Numerous algorithms, presented in the bibliography, may be used to solve this problem.[22,23]

At the end of each time increment t_{i+1}, these algorithms yield:

(a) a finite element displacement field that satisfies the kinematic constraints:

$$U_h(t_{i+1}, M) = \mathbf{N}(M)\mathbf{q}(t_{i+1}) \tag{3}$$

where $\mathbf{N}(M)$ denotes the matrix of the shape functions and $\mathbf{q}(t_{i+1})$ the vector of the nodal displacement at t_{i+1};

(b) a stress field $\sigma_h(t_{i+1}, M)$ that satisfies the equilibrium equation for the finite element problem at t_{i+1}:

$$\forall U_h^* = \mathbf{N}(M)\mathbf{q}^* \text{ such that } U_h^* = 0 \text{ on } \partial_1\Omega$$
$$\int_\Omega \sigma_h(t_{i+1}, M)^T \mathbf{B}(M)\mathbf{q}^* \, d\Omega = \int_\Omega f_d(t_{i+1}, M)^T \mathbf{N}(M)\mathbf{q}^* \, d\Omega + \int_{\partial_2\Omega} F_d(t_{i+1}, M)^T \mathbf{N}(M)\mathbf{q}^* \, dS \tag{4}$$

where $\mathbf{B}(M)\mathbf{q}^*$ is the strain associated with the field $U_h^* = \mathbf{N}(M)\mathbf{q}^*$.

Remarks. 1. In practice, the field $\sigma_h(t_{i+1}, M)$ is only computed on the integration points of each finite element.

2. The stress field given by the finite element solver is very often the field $\tilde{\sigma}_h(t_{i+1}, M)$ obtained from $\varepsilon(U_h)$ by integrating the constitutive relation:

$$\tilde{\sigma}_h(t_{i+1}, M) = \mathbf{A}(\varepsilon(U_h(\tau, M)), \tau \leqslant t_{i+1}) \tag{5}$$

It must be noticed that this stress field satisfies equation (4) in an approximate manner.

Drucker's inequality

Let (ε, σ) and $(\bar{\varepsilon}, \bar{\sigma})$ be two strain–stress pairs, with ε and $\bar{\varepsilon}$ related to σ and $\bar{\sigma}$ through the constitutive relation, and with ε and $\bar{\varepsilon}$ equal to zero in the initial state. The material strictly satisfies Drucker's inequality if

$$\int_0^t (\sigma - \bar{\sigma})^T (\dot{\varepsilon} - \dot{\bar{\varepsilon}}) \, d\tau \geqslant 0 \quad \forall t \in [0, T] \tag{6}$$

and

$$\int_0^t (\sigma - \bar{\sigma})^T (\dot{\varepsilon} - \dot{\bar{\varepsilon}}) \, d\tau = 0 \quad \forall t \in [0, T] \Rightarrow \{\varepsilon = \bar{\varepsilon} \text{ and } \sigma = \bar{\sigma}\} \tag{7}$$

Most of the constitutive laws used in plasticity and in viscoplasticity strictly satisfy Drucker's inequality, as does the Prandtl–Reuss model which will be used for the examples.

Error in constitutive relation

Let (U_{CA}, σ_{SA}) be a displacement–stress pair, which is zero at $t = 0$. U_{CA} is a kinematically admissible displacement field (2a), and σ_{SA} satisfies the equilibrium equation (2b). Generally, this pair does not satisfy the constitutive relation (2c). Thus, (U_{CA}, σ_{SA}) is an approximate solution to the problem (2).

The strain field $\varepsilon_{CA} = \varepsilon(U_{CA})$ can be related to a stress field σ_{CA} through the constitutive relation. In the same way, the stress σ_{SA} can be related to a strain field ε_{SA} through the inverse of the constitutive relation.

We define the quantity $\eta(t, M)$ as follows:

$$\eta(t, M) = \int_0^t (\sigma_{SA} - \sigma_{CA})^T (\dot{\varepsilon}_{SA} - \dot{\varepsilon}_{CA}) \, d\tau \tag{8}$$

For a material which strictly satisfies Drucker's inequality, the pair (U_{CA}, σ_{SA}) is the exact solution of the problem (2), if and only if

$$\eta(t, M) = 0 \quad \forall t \in [0, T] \quad \text{and} \quad \forall M \in \Omega \tag{9}$$

To estimate the quality of (U_{CA}, σ_{SA}) as an approximate solution to problem (2), the previous relations lead us to define the following error measure:

$$\mathbf{e} = \left[\operatorname*{Sup}_{t \in [0, T]} \int_{\Omega} \eta(t, M) \, d\Omega \right]^{1/2} \tag{10}$$

so that

$$\mathbf{e} = 0 \Leftrightarrow (U_{CA}, \sigma_{SA}) \text{ is the exact solution to problem (2)} \tag{11}$$

$\mathbf{e}$ is called the error in constitutive relation associated with the admissible pair (U_{CA}, σ_{SA}).

Associated with this absolute global error, we define a relative global error:

$$\varepsilon = \frac{\mathbf{e}}{D} \tag{12}$$

where

$$D = \left[2 \operatorname*{Sup}_{t \in [0, T]} \int_{\Omega} \int_0^t (\sigma_{SA}^{\mathrm{T}} \dot{\varepsilon}_{SA} + \sigma_{CA}^{\mathrm{T}} \dot{\varepsilon}_{CA}) \, d\tau \, d\Omega \right]^{1/2}$$

We also define the contribution of a time interval $[0, t]$ to the relative error:

$$\varepsilon_{[0,t]} = \frac{[\operatorname{Sup}_{\tau \in [0,t]} \int_{\Omega} \eta(\tau, M) \, d\Omega]^{1/2}}{D} \tag{13}$$

the contribution at t:

$$\varepsilon(t) = \frac{[\int_{\Omega} \eta(t, M) \, d\Omega]^{1/2}}{D} \tag{14}$$

and the contribution of the element E at t:

$$\varepsilon_E(t) = \frac{[\int_E \eta(t, M) \, d\Omega]^{1/2}}{D} \tag{15}$$

Obviously, these contributions satisfy

$$\varepsilon^2(t) = \sum_E \varepsilon_E^2(t) \quad \text{and} \quad \varepsilon = \operatorname*{Sup}_{t \in [0, T]} \varepsilon(t) \tag{16}$$

Remark. The quantity $\int_{\Omega} \int_0^t (\sigma_{SA}^{\mathrm{T}} \dot{\varepsilon}_{SA} + \sigma_{CA}^{\mathrm{T}} \dot{\varepsilon}_{CA}) \, d\tau \, d\Omega$, which is used for the definition of D, is always greater than or equal to zero. This quantity is greater than zero if one of the fields, σ_{SA} or σ_{CA}, is not equal to zero. Indeed, it is equal to the sum of

$$\int_0^t (\sigma_{SA} - 0)^{\mathrm{T}} (\dot{\varepsilon}_{SA} - 0) \, d\tau \quad \text{and} \quad \int_0^t (\sigma_{CA} - 0)^{\mathrm{T}} (\dot{\varepsilon}_{CA} - 0) \, d\tau \tag{17}$$

quantities which are always positive or equal to zero as a consequence of Drucker's inequality. At least one of these quantities is not zero if σ_{SA} or σ_{CA} is not equal to zero.

Relation with the error in elasticity

Let us suppose that the whole structure remains elastic or that we do not introduce plasticity. We can therefore write

$$\varepsilon_{SA} = K_e^{-1}\sigma_{SA} \quad \text{and} \quad \sigma_{CA} = K_e\varepsilon_{CA} \tag{18}$$

where K_e denotes the Hooke matrix.

By integrating (8) over the time interval $[0, t]$, we obtain

$$\eta(t, M) = \tfrac{1}{2}[\sigma_{SA}(t) - K_e\varepsilon_{CA}(t)]^{\mathrm{T}} K_e^{-1}[\sigma_{SA}(t) - K_e\varepsilon_{CA}(t)] \tag{19}$$

and hence

$$\mathbf{e}^2_{\text{elasticity}} = \int_\Omega \eta(T, M)\,\mathrm{d}\Omega = \tfrac{1}{2}\,\|\sigma_{SA}(T) - K_e\varepsilon_{CA}(T)\|^2 \tag{20}$$

where $\|\cdot\|$ is the energy norm over the whole structure.
In the same way, we obtain

$$D^2 = [\,\|\sigma_{SA}(T)\|^2 + \|K_e\varepsilon_{CA}(T)\|^2] \tag{21}$$

hence

$$\varepsilon_{\text{elasticity}} = \left[\frac{1}{2}\frac{\|\sigma_{SA}(T) - K_e\varepsilon_{CA}(T)\|^2}{\|\sigma_{SA}(T)\|^2 + \|K_e\varepsilon_{CA}(T)\|^2}\right]^{1/2} \tag{22}$$

When the whole structure remains elastic, the error in constitutive relation defined in (12) is equal to the energy errors classically used.[4, 24]

Relation with the exact error

It may be shown that in elasticity the error in constitutive relation classically used is always greater than or equal to the exact error. And, it has been shown by numerical experiments that, for classical construction of the admissible fields, the effectivity index $\theta_{\text{effectivity}}$ is approximately equal to 1·5 (Reference 25) where

$$\theta_{\text{effectivity}} = \frac{\text{computed error}}{\text{exact error}}$$

Thus, the error based on Drucker's inequality has the same properties as long as the structure remains elastic.

Some numerical experiments have been conducted in elastoplasticity, and we observe that in general $\theta_{\text{effectivity}}$ varies between 1·5 and 4.

APPLICATION TO FINITE ELEMENT COMPUTATION

The displacement fields $U_h(t_i, M)$, obtained by a finite element computation, satisfy the kinematic constraints. Under the assumption that the displacement field $U_d(t, M)$ given on $\partial_1\Omega$ is linear on each time increment $[t_i, t_{i+1}]$, assumption which is not very restrictive in practice, the field U_{CA} can be chosen for $t \in [t_i, t_{i+1}]$ equal to

$$U_{CA}(t, M) = U_h(t_i, M) + \frac{t - t_i}{t_{i+1} - t_i}(U_h(t_{i+1}, M) - U_h(t_i, M)) \tag{23}$$

However, the calculated stress σ_h is not statistically admissible. So, it is necessary to build, with a post-processor of the finite element analysis, a stress field σ_{SA} that satisfies the equilibrium equations over the interval $[0, T]$.

This construction is conducted in two steps: In the first step, we compute, at the end of each time step, a stress field $\sigma_{SA}(t_{i+1})$ that satisfies the equilibrium equations at t_{i+1}. In the second step, the stress field σ_{SA} is built at any time by interpolation.

Construction of σ_{SA}

Over the past several years, we have developed techniques for constructing admissible fields for the evaluation of errors in linear analysis. These techniques are completely independent of the constitutive relation; they will be used herein to build, at the end of each time step t_{i+1}, a stress field $\sigma_{SA}(t_{i+1})$ that satisfies the equilibrium equations. We briefly recall the main ideas of this construction in the Appendix; for more details the reader may consult Ladevèze *et al.*[4, 24]

Using the field $\sigma_h(t_{i+1}, M)$, the procedure described in the Appendix allows obtaining, at the end of each increment, a field $\sigma_{SA}(t_{i+1}, M)$ that satisfies the equilibrium equations (2b) at t_{i+1}. Then, if we define for $t \in [t_i, t_{i+1}]$:

$$\sigma_{SA}(t, M) = \sigma_{SA}(t_i, M) + \frac{t - t_i}{t_{i+1} - t_i}[\sigma_{SA}(t_{i+1}, M) - \sigma_{SA}(t_i, M)] \tag{24}$$

and under the assumption that the loading is linear on each time increment, an assumption which is not very restrictive in practice, we obtain a field σ_{SA} that satisfies the equilibrium equations (2b) at each moment.

Remark. The procedure for constructing $\sigma_{SA}(t_{i+1}, M)$ uses the equilibrium equation of the finite element model (4) which is verified by $\sigma_h(t_{i+1}, M)$.

If the finite element software gives the field $\tilde{\sigma}_h(t_{i+1}, M)$ defined by (5), which satisfies (4) only approximately, it is necessary to build a field $\sigma_h(t_{i+1}, M)$ which satisfies (4) exactly. Such a field can easily be computed in a post-processor by partially performing an additional iteration of Newton's method. More precisely, the field $\sigma_h(t_{i+1}, M)$ is chosen to be equal to

$$\sigma_h(t_{i+1}, M) = \tilde{\sigma}_h(t_{i+1}, M) + K_e \mathbf{B}(M) \Delta\tilde{\mathbf{q}} \tag{25}$$

where $\Delta\tilde{\mathbf{q}}$ is the solution to the linear problem:

$$K_e \Delta\tilde{\mathbf{q}} = \Delta\mathbf{F} \tag{26}$$

where

$$\mathbf{K}_e = \int_\Omega \mathbf{B}(M)^T K_e \mathbf{B}(M)\, d\Omega$$

and

$$\Delta\mathbf{F} = \int_\Omega \mathbf{N}(M)^T f_d(t_{i+1}, M)\, d\Omega + \int_{\partial_2\Omega} \mathbf{N}(M)^T F_d(t_{i+1}, M)\, dS - \int_\Omega \mathbf{B}(M)^T \tilde{\sigma}_h(t_{i+1}, M)\, d\Omega$$

In (25), instead of Hooke's matrix K_e, any symmetric definite positive matrix may be used.

Computation of the error in constitutive relation

When the pair (U_{CA}, σ_{SA}) is known, it is necessary to determine the fields σ_{CA} and ε_{SA} by integrating the constitutive law, in order to compute the error in constitutive relation. On each Gauss integration point over the whole structure, we integrate the constitute law:

(i) for a known history of strain $\varepsilon(U_{CA})$ to obtain the history of stress σ_{CA};
(ii) for a known history of stress σ_{SA} to obtain the history of strain ε_{SA}.

Integrating the constitutive law is conducted by classical methods.[26-28] However, in order to obtain an accurate estimation of $\eta(t, M)$ and hence of the error in constitutive relation, integration is carried out on a sub-discretization of the discretization used for the incremental method. In practice, each time step $[t_i, t_{i+1}]$ is subdivided into m regular sub-increments $[t'_j, t'_{j+1}]$ where $t'_0 = t_i$ and $t'_m = t_{i+1}$, and we choose $m \approx 5$–20 depending on the size of the time step.

TIME ERROR INDICATOR

The error measure ε derived from Drucker's inequality is global in space and in time. It takes into account the errors due to the mesh as well as the errors due to the time discretization. To develop efficient adaptivity techniques, it is generally insufficient to control only the size of the elements of the mesh, it is also necessary to control the size of the time steps. To achieve this goal, it is essential to be able to separate, in the global error ε, the part of the error due to the spatial discretization from the part of the error due to the time discretization. To solve this difficulty, we propose here a very simple time error indicator which allows us to estimate the part of the error due to the time discretization.

Let us consider the pair (U_{CA}, σ_h), where U_{CA} is obtained from the finite element solution by (23), and where σ_h is the stress field defined by

$$\forall t \in [t_i, t_{i+1}] \quad \sigma_h(t, M) = \sigma_h(t_i, M) + \frac{t - t_i}{t_{i+1} - t_i} [\sigma_h(t_{i+1}, M) - \sigma_h(t_i, M)] \tag{27}$$

where the fields $\sigma_h(t_{i+1}, M)$ satisfy, at the end of each increment, the equilibrium equation of the finite element model (4).

Let us consider the problem (28) obtained from the reference problem (2) by a finite element spatial discretization: *Find* $U_h(t, M) = \mathbf{N}(M)\mathbf{q}(t)$ *and* $\sigma_h(t, M)$ *such that*:

U_h *satisfies the kinematic constraints*:

$$\forall t \in [0, T] \quad U_h(t, M) = U_d(t, M) \quad \text{on } \partial_1\Omega \tag{28a}$$

σ_h *satisfies the equilibrium equations of the finite element model* $\forall t \in [0, T]$:

$$\begin{aligned} &\forall U_h^*(M) = \mathbf{N}(M)\mathbf{q}^* \quad \text{such that } U_h^* = 0 \quad \text{on } \partial_1\Omega \\ &\int_\Omega \sigma_h(t, M)^{\mathrm{T}} \mathbf{B}(M)\mathbf{q}^* \, \mathrm{d}\Omega = \int_\Omega f_d(t, M)^{\mathrm{T}} \mathbf{N}(M)\mathbf{q}^* \, \mathrm{d}\Omega + \int_{\partial_2\Omega} F_d(t, M)^{\mathrm{T}} \mathbf{N}(M)\mathbf{q}^* \, \mathrm{d}S \end{aligned} \tag{28b}$$

σ_h *and the strain* $\varepsilon(U_h)$ *satisfy the constitutive relation*:

$$\forall t \in [0, T] \quad \sigma_h(t, M) = \mathbf{A}[\varepsilon(U_h)(t', M), t' \leqslant t] \quad \text{in } \Omega \tag{28c}$$

at $t = 0$, *the structure is in its natural state*:

$$\mathbf{q}(0) = 0, \quad \sigma_h(0, M) = 0 \tag{28d}$$

The pair (U_{CA}, σ_h) so constructed satisfies all the equations of problem (28), except the constitutive relation (28c). The quality of this pair as an approximate solution to problem (28) may be estimated by an error measure built in Drucker's inequality.

Let ε_h be a strain field computed from σ_h by an integration of the constitutive law. Then the pairs $(\varepsilon_h, \sigma_h)$ and $(\varepsilon(U_{CA}), \sigma_{CA})$ satisfy the constitutive law. The associated error in constitutive law is defined by

$$\mathbf{i}_{\text{time}} = \left[\operatorname*{Sup}_{t \in [0,T]} \int_\Omega \bar{\eta}(t, M)\, d\Omega \right]^{1/2} \tag{29}$$

where

$$\bar{\eta}(t, M) = \int_0^t (\sigma_h - \sigma_{CA})^{\mathrm{T}} (\dot{\varepsilon}_h - \dot{\varepsilon}(U_{CA}))\, d\tau \tag{30}$$

Condition (7) shows that $\mathbf{i}_{\text{time}} = 0$ if and only if the pairs $(\varepsilon_h, \sigma_h)$ and $(\varepsilon(U_{CA}), \sigma_{CA})$ are equal, that is if and only if the pair (U_{CA}, σ_h) is the exact solution to problem (28). Hence, for a given spatial discretization, $\mathbf{i}_{\text{time}}$ estimates the errors due to the time discretization: incremental method errors and Newton's algorithm errors.

The absolute error $\mathbf{i}_{\text{time}}$ can be associated, as for $\mathbf{e}$, with a relative error:

$$i_{\text{time}} = \frac{\mathbf{i}_{\text{time}}}{D_{\text{time}}} \tag{31}$$

with

$$D_{\text{time}} = \left[2 \operatorname*{Sup}_{t \in [0,T]} \int_\Omega \int_0^t (\sigma_{CA}^{\mathrm{T}} \varepsilon_{CA} + \sigma_h^{\mathrm{T}} \dot{\varepsilon}(U_h))\, d\tau\, d\Omega \right]^{1/2}$$

We also define the contribution of time interval $[0, t]$ to the relative error:

$$i_{\text{time},[0,t]} = \frac{[\operatorname{Sup}_{\tau \in [0,t]} \int_\Omega \bar{\eta}(\tau, M)\, d\Omega]^{1/2}}{D_{\text{time}}} \tag{32}$$

the contribution at t:

$$i_{\text{time}}(t) = \frac{[\int_\Omega \bar{\eta}(t, M)\, d\Omega]^{1/2}}{D_{\text{time}}} \tag{33}$$

and the contribution of an element E at t:

$$i_{\text{time},E}(t) = \frac{[\int_\Omega \bar{\eta}(t, M)\, d\Omega]^{1/2}}{D_{\text{time}}} \tag{34}$$

Obviously, these contributions satisfy

$$i_{\text{time}}^2(t) = \sum_E i_{\text{time},E}^2(t) \quad \text{and} \quad i_{\text{time}} = \operatorname*{Sup}_{t \in [0,T]} i_{\text{time}}(t) \tag{35}$$

Hence, i_{time} estimates the quality of the solution computed as an approximate solution to problem (28).

In practice, we will use $\mathbf{i}_{\text{time}}$ or the relative quantity i_{time} as an error indicator to evaluate the part of the error due to the time discretization. In the fifth part of this paper, we will show that the knowledge of the error $\mathbf{e}$ and of the time indicator $\mathbf{i}_{\text{time}}$ allows constructing an indicator to evaluate the part of the error due to space.

EXAMPLES

Three examples of evaluating error measures are presented herein. The finite element analyses are 2-D or axisymmetric analyses computed with the finite element software CASTEM2000.[29] The meshes used are pre-optimized in elasticity,[24,25] and they are generated by our automatic 2-D mesh generator ARAIGNEE.

Example 1

The first example is the computation of a perforated disc (Figure 2(a)) which is subjected, in its upper and lower parts, to a monotonous loading (Figure 2(b)). The initial mesh has 415 3-node triangular elements (Figure 2(c)) and the analysis is conducted with 23 time steps. The global error computed is $\varepsilon = 13$ per cent, and the time error indicator is $i_{\text{time}} = 0{\cdot}3$ per cent. Figure 2(d) shows the evolution of the computed contributions as functions of the time $\varepsilon_{[0,t]}$ and $i_{\text{time},[0,t]}$. Figure 2(e) shows the size of the plastic zone at the end of the loading, and Figure 2(f) shows the map of the contributions $\varepsilon_E(t_m)$ at t_m when $\int_\Omega \eta(t, M)\,d\Omega$ is maximum; for this example, $t_m = T$.

In this example, the whole structure remains elastic up to $t = 40$. When $t \leqslant 40$, Figure 2(d) displays that the evolution of $\varepsilon_{[0,t]}$ is linear with respect to the loading, which corresponds with a constant error in elasticity. During the elastic loading, it can also be noticed that $i_{\text{time},[0,t]}$ is zero, which is normal because during an elastic loading, time does not play any part.

Example 2

The second example is an axisymmetric analysis conducted with 6-node triangular elements. The problem is described in Figure 3(a); it is an axially symmetric part of a press which is subjected to a non-monotonous loading (Figure 3(b)). Thirty-five time steps are used to determine the time discretization. The evolution over time of the contributions $\varepsilon_{[0,t]}$ and $i_{\text{time},[0,t]}$ are given in Figure 3(c). As in the first example, $i_{\text{time},[0,t]}$ is zero during elastic loading. Moreover, during the two phases of 'elastic unloading', the contributions $\varepsilon_{[0,t]}$ and $i_{\text{time},[0,t]}$ remain constant.

The mesh, optimized in elasticity, contains 211 triangular elements (Figure 3(d)). The following figures show the map of the contributions $\varepsilon_E(t)$ at different time steps:

Figure 3(e): at time step t_e, where the whole structure is elastic;
Figure 3(f): at time step t_1, where the first cycle of loading is maximum;
Figure 3(g): at time step t_2, where the second cycle of loading is maximum.

Finally, Figures 2(h) and 2(i) show the plastic zone at t_1 and t_2.

Example 3

The aim of the third example is to compare on regular meshes the efficiency of the 3- and 6-node triangular elements. The mechanical problem is shown in Figure 4(a). It is a bending beam computed in plane stress.

The loading is monotonous and the applied loads are a density of forces:

$$\vec{F}_0 = \lambda(t)[2Ly\,\vec{x} + (y^2 - h^2)\,\vec{y}] \quad \text{on } x = 0$$

$$\vec{F}_L = \lambda(t)\,[(h^2 - y^2)\,\vec{y}] \quad \text{on } x = L$$

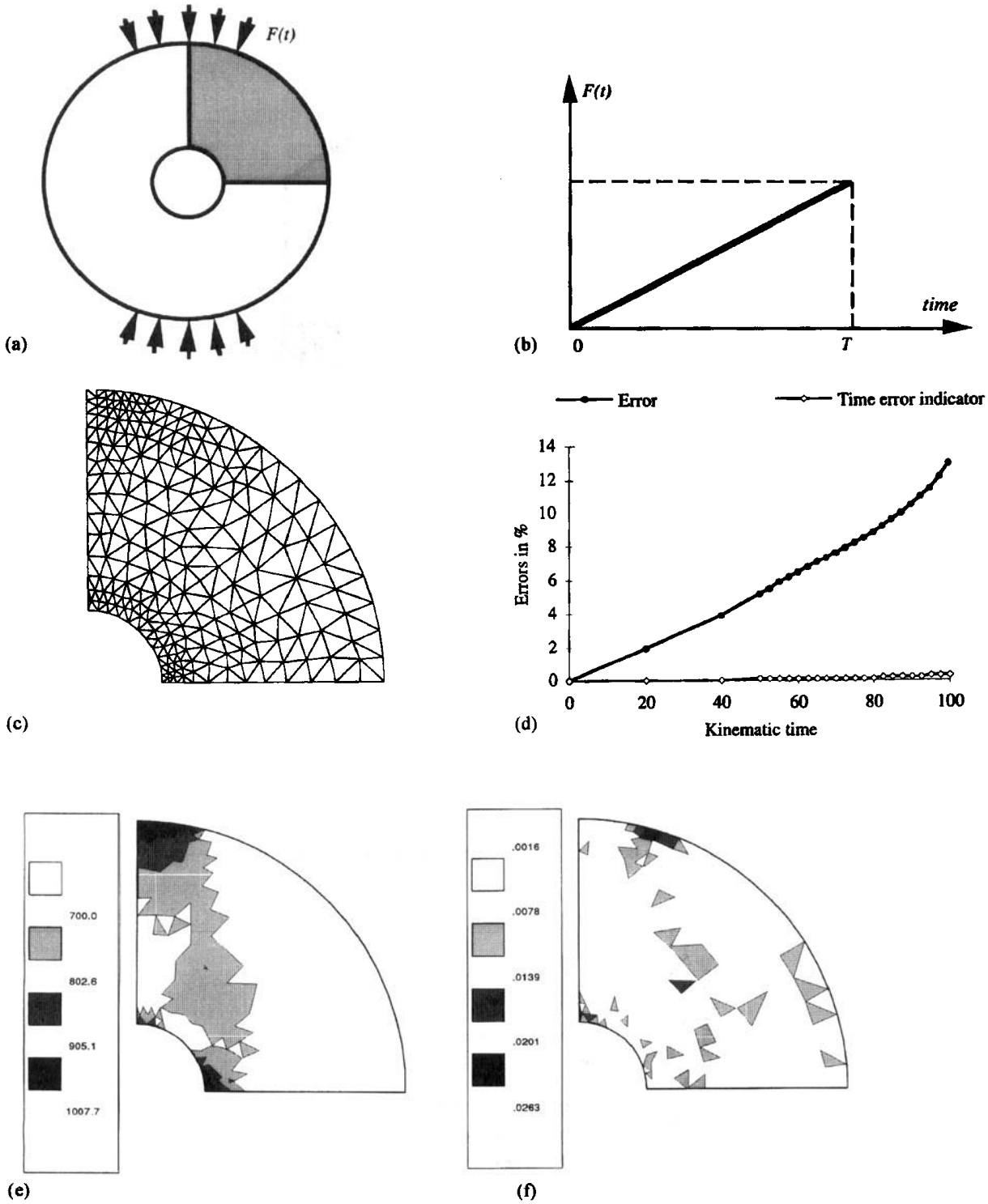

Figure 2. Computation of a perforated disc (a) Mechanical problem (b) Monotonous loading (c) Mesh, 415 3-node elements—240 nodes (d) Contributions $\varepsilon_{[0,t]}$ and $i_{\text{time},[0,t]}$ $\varepsilon = 13$ per cent, $i_{\text{time}} = 0{\cdot}3$ per cent (e) Size of the plastic zone, initial threshold 700 MPa (f) Local error contributions

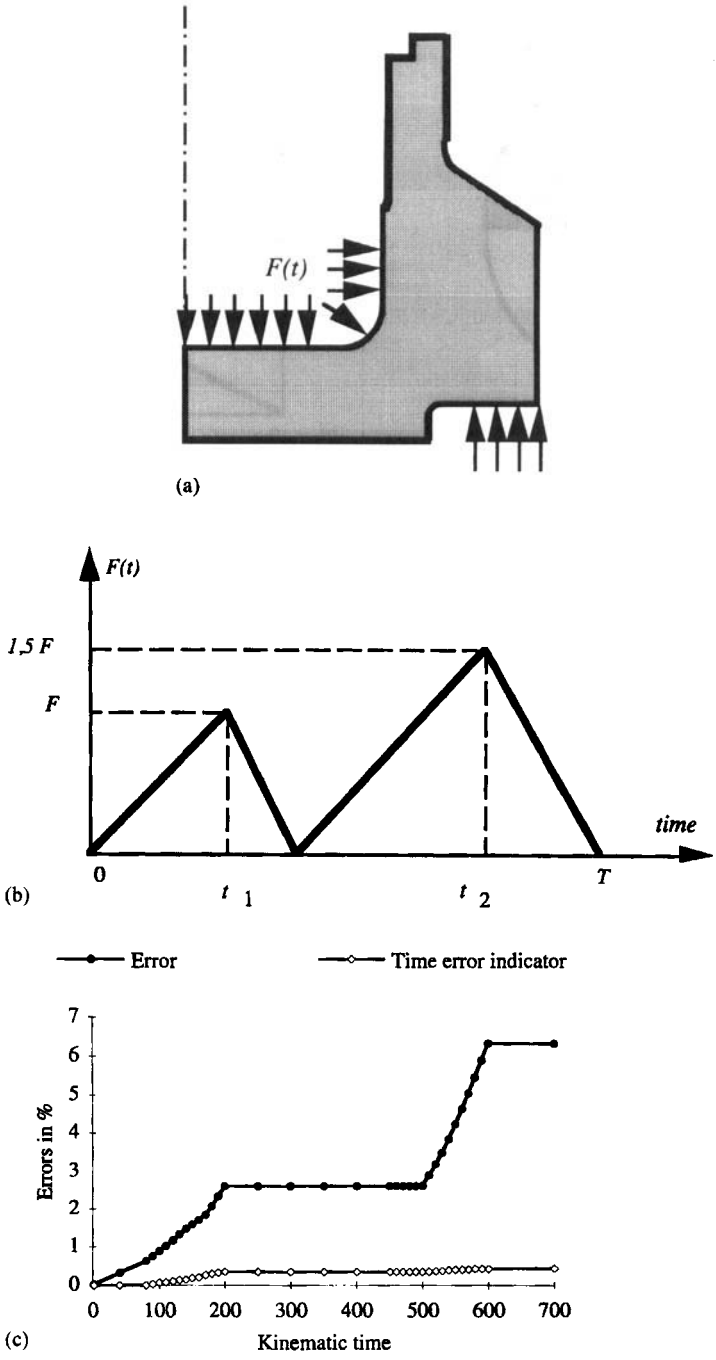

Figure 3. Computation of an axially symmetric press (a) Mechanical problem (b) Non-monotonous loading (c) Contributions $\varepsilon_{[0,t]}$ and $i_{\text{time},[0,t]}$, $\varepsilon = 6{\cdot}3$ per cent, $i_{\text{time}} = 0{\cdot}43$ per cent (d) Mesh, 211 6-node triangular elements—486 nodes (e) Local error contributions at t_e (f) Local error contributions at t_1 (g) Local error contributions at t_2 (h) Size of the plastic zone at t_1, initial threshold 400 MPa (i) Size of the plastic zone at t_2 initial threshold 400 MPa

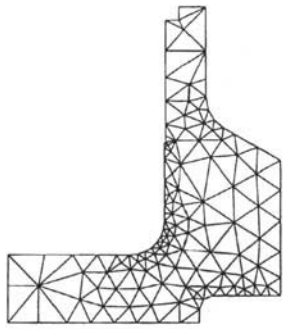

(d)

(e)

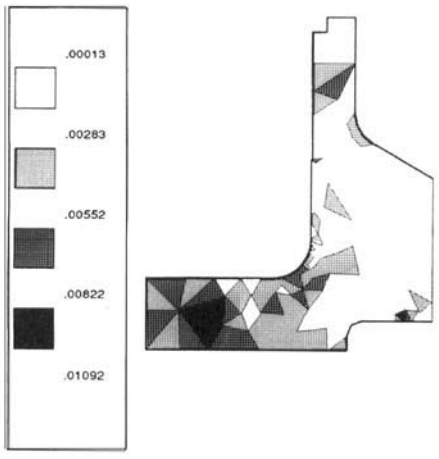

(f)

(g)

(h)

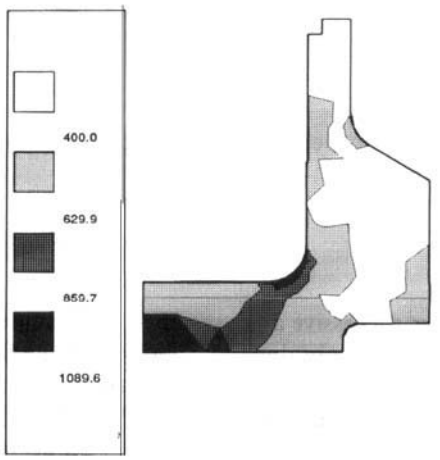

(i)

Figure 3. (d–i)

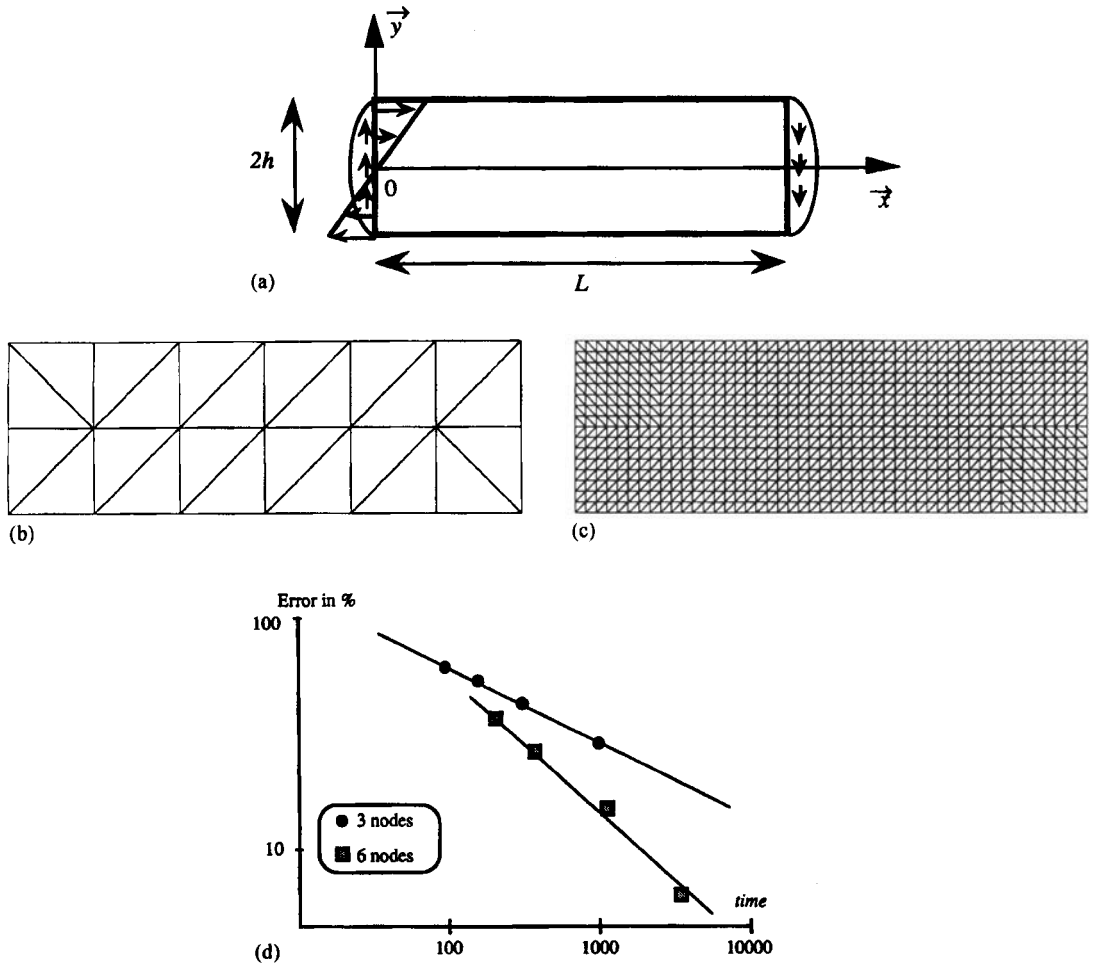

Figure 4. Comparison of the efficiencies of 3-node triangular elements with 6-node triangular elements (a) Mechanical problem (b) 24-element mesh (c) 1536-element mesh (d) Global relative errors computed as a function of computer processing time

It is easy to verify that, during elastic loading, the exact stress solution is a second-degree polynomial:

$$\sigma_{xx} = \lambda(t)[2(x - L)y], \quad \sigma_{xy} = \lambda(t)[h^2 - y^2], \quad \sigma_{yy} = 0$$

Four successive analyses have been conducted on the mesh shown in Figure 4(b) and on three other meshes obtained by subdividing the first one. The finest mesh is shown in Figure 4(c). The global relative errors computed are shown in Figure 4(d) as a function of the time necessary for finite element analysis on an HP 5500 workstation.

It should be noted that for a given accuracy, the use of 6-node triangular elements leads to a five-fold time saving in comparison with the use of 3-node triangular elements.

ADAPTATIVITY OF COMPUTATIONS

To control the parameters of an elastoplastic computation, it is necessary to separate, in the global error, the part due to the time discretization from the part due to the space discretization. Moreover, to accurately predict the parameters of the final FE analysis from the results of an initial FE analysis, we must identify the behaviour of the errors used as a function of the size h of the elements and of the size Δt of the time increments. As far as we know, theoretical results on this subject do not exist; so, we have estimated these types of behaviour with numerical tests.

Study of the time error indicator

Let us once again consider the beam problem (Figure 4(a)). An initial finite element analysis is conducted on the mesh of Figure 5(a) with 6-node triangular elements and 18 time steps. The global error computed is $\varepsilon = 1{\cdot}60$ per cent, and the time error indicator is $i_{\text{time}} = 0{\cdot}50$ per cent. The evolution over time of the contributions $\varepsilon_{[0,t]}$ and $i_{\text{time},[0,t]}$ is given in Figure 5(b), and the size of the plastic zone is given in Figure 5(c).

With a coarser time discretization (6 time steps), the errors computed are (Figure 5(d))

$$\varepsilon = 2{\cdot}39 \text{ per cent} \quad \text{and} \quad i_{\text{time}} = 2{\cdot}05 \text{ per cent}$$

With the same time discretization of 6 time steps and a refined mesh (each element of the initial mesh being subdivided into 4 elements), the errors computed are (Figure 5(e))

$$\varepsilon = 2{\cdot}11 \text{ per cent} \quad \text{and} \quad i_{\text{time}} = 2{\cdot}06 \text{ per cent}$$

This example shows, on the one hand, that if the time discretization is coarse and the mesh is very fine, the global error is very similar to the time error indicator and, on the hand, that the time error indicator, for a given time discretization, depends very little on the mesh used. We have also noticed that during the elastic phases (where there is no time integration), this indicator is zero. These observations lead us to consider that i_{time} is a good estimate of the part of the global error due to the time discretization.

To evaluate the behaviour of i_{time} as a function of the time step size Δt, we have conducted some numerical tests which show that

$$i_{\text{time}} = O(\Delta t) \tag{36}$$

As an example, let us consider the console shown in Figure 6(a). The mesh used (273 6-node triangular elements) is given in Figure 6(b), and the loading is monotonous. The analysis is conducted for various values of the number of time steps. The evolution of i_{time} as a function of the number of time steps is shown in Figure 6(c), and the size of the plastic zone is given in Figure 6(d). It can be noticed that the evolution of i_{time} as a function of the number of time steps is consistent with condition (36).

Evolution of the error as a function of h

The error $\mathbf{e}$ takes into account the errors due to the mesh as well as those due to the time discretization. To separate these contributions, we suppose that the global error $\mathbf{e}$ may be split into two parts:

$$\mathbf{e}^2 = \mathbf{I}^2_{\text{space}} + \mathbf{I}^2_{\text{time}} \tag{37}$$

where $\mathbf{I}_{\text{space}}$ denotes the contribution of the errors due to the spatial discretization and $\mathbf{I}_{\text{time}}$ the contribution of the errors of discretization over time.

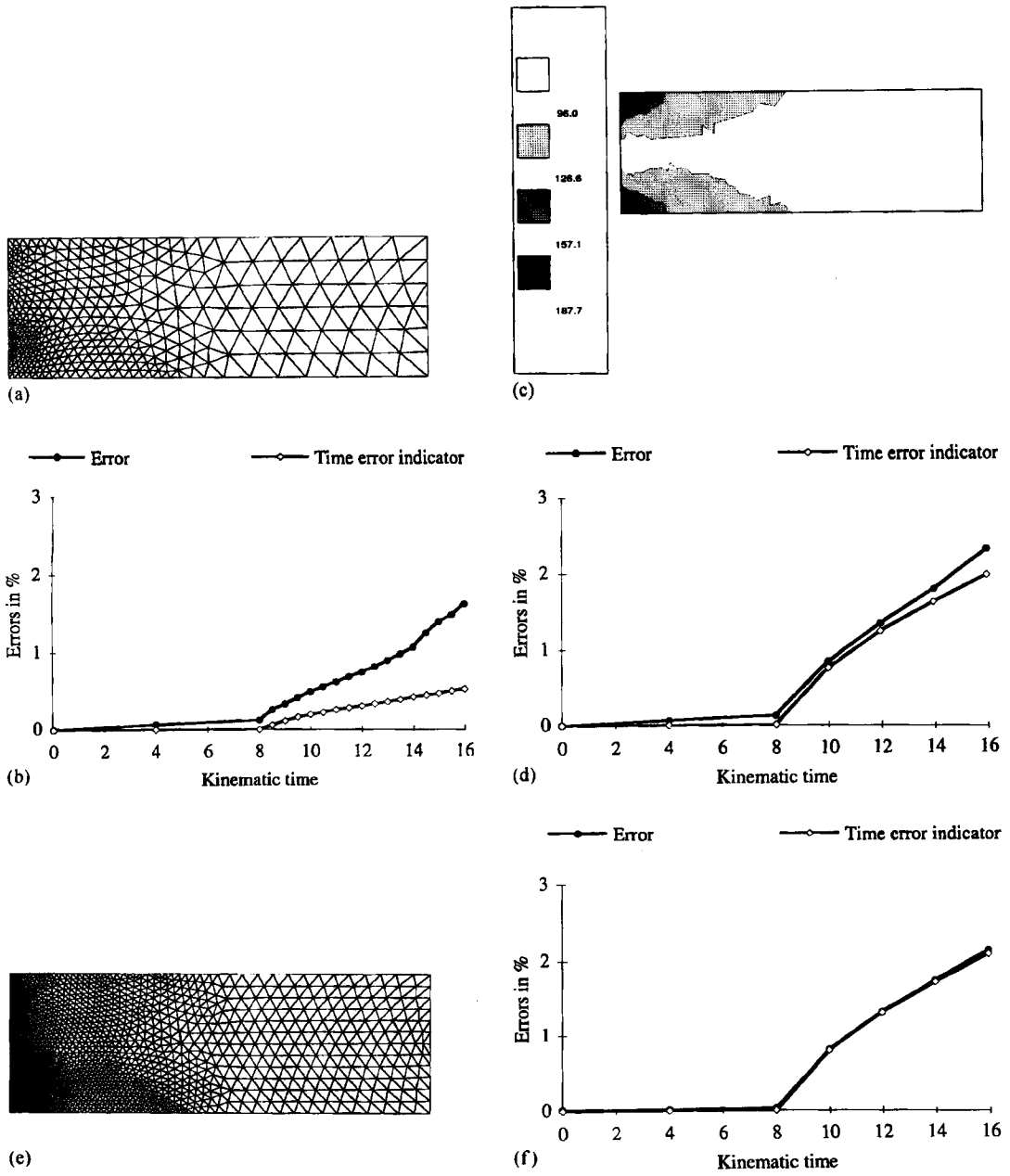

Figure 5. Study of the time error indicator (a) Mesh 1, 778 6-node triangular elements—1645 nodes (c) Size of the plastic zone, initial threshold 96 MPa (b) Contributions $\varepsilon_{[0,t]}$ and $i_{\text{time},[0,t]}$, 18 increments, mesh 1 (d) Contributions $\varepsilon_{[0,t]}$ and $i_{\text{time},[,t]}$ 6 increments mesh 1 (e) Mesh 2, 3112 6—node triangular elements—6401 nodes (f) Contributions $\varepsilon_{[0,t]}$ and $i_{\text{time},[0,t]}$, 6 increments, mesh 2

Considering the properties noted previously, the time indicator $\mathbf{i}_{\text{time}}$ (29) is a good estimate of $\mathbf{I}_{\text{time}}$. Thus, the part of the error due to space may be defined by

$$\mathbf{I}^2_{\text{space}} = \text{Sup}\{\mathbf{e}^2 - \mathbf{i}^2_{\text{time}}, 0\} \tag{38}$$

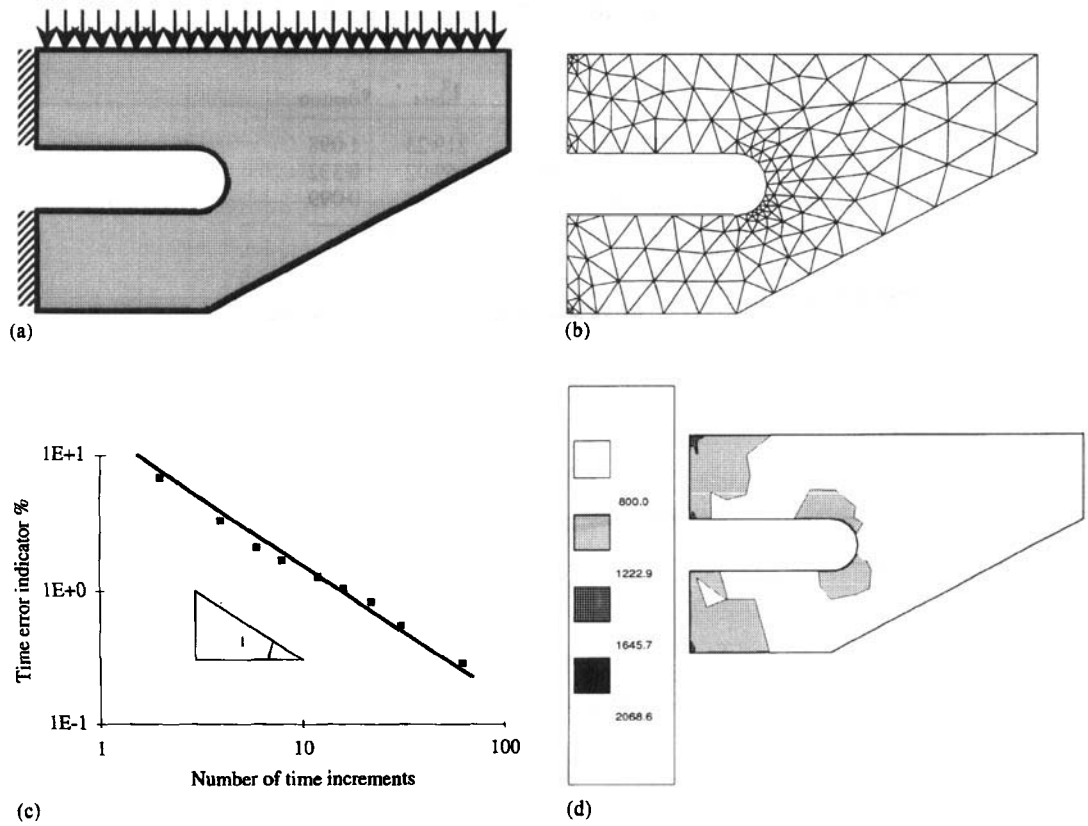

Figure 6. Evolution of the time error indicator as a function of the number of time steps (a) Mechanical problem (b) Mesh, 273 6-node triangular elements—618 nodes (c) Evolution of i_{time} (d) Size of the plastic zone, initial threshold 800 MPa

Remark. For each of the examples studied, we have always noted the inequality $\mathbf{e}^2 > \mathbf{i}^2_{time}$. If this inequality holds, we have $\mathbf{I}^2_{space} = \mathbf{e}^2 - \mathbf{i}^2_{time}$. Nevertheless, as the inequality $\mathbf{e}^2 > \mathbf{i}^2_{time}$ has not been proved, definition (38) ensures that $\mathbf{I}^2_{space}$ is greater than or equal to zero.

To be able to predict new sizes for the elements during an adaptation procedure, it is necessary to know, at least approximately, the evolution of $\mathbf{I}_{space}$ as a function of h. The aim of the following examples is to evaluate this evolution.

In the first example, let us reconsider the perforated disc shown in Figure 2(a) and a 415 3-node element mesh (Figure 2(c)). Two other meshes are obtained by subdividing this first mesh. In a first step, we have performed, on each mesh, a finite element analysis in elasticity, and we have computed $\mathbf{e}_{elasticity}$ (20), the error in constitutive relation classically used in linear analysis.[24] In a second step, we have performed the same analyses for an elastoplastic constitutive relation, with the monotonous loading shown in Figure 2(b), and we have computed $\mathbf{e}$, $\mathbf{i}_{time}$ and $\mathbf{I}_{space}$. The results are shown in Table I and in Figure 7 for $\mathbf{I}^2_{space}$ and $\mathbf{e}^2_{elasticity}$.

It can be noted that the indicator in space $\mathbf{I}_{space}$ and the error in elasticity $\mathbf{e}_{elasticity}$ have a similar evolution. More precisely, on the two finer meshes, we obtain

$$\mathbf{I}_{space} = O(h^{0.84}) \quad \text{and} \quad \mathbf{e}_{elasticity} = O(h^{0.87})$$

Table I. Results for 3-node triangular elements

Number of elements	e^2	i^2_{time}	I^2_{space}	$e^2_{elasticity}$
415	219·34	0·11	219·23	1·098
1660	70·05	0·13	69·92	0·332
6640	22·00	0·12	21·88	0·099

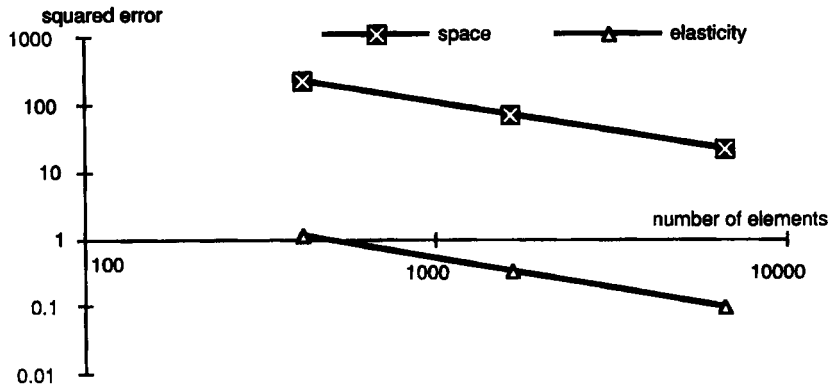

Figure 7. Evolution of I^2_{space} and $e^2_{elasticity}$ as a function of the number of elements

The convergence rate obtained for I_{space} with 3-node triangular elements is thus similar to the one obtained in elasticity. A similar computation with 6-node triangular elements yields the results of Table II.

Figure 8 shows similar evolutions for I^2_{space} and $e^2_{elasticity}$. More precisely, on the two finer meshes, we obtain

$$I_{space} = O(h^{0.93}) \quad \text{and} \quad e_{elasticity} = O(h^{0.96})$$

Again, the rates of convergence of the indicator in space I_{space} and the error in elasticity $e_{elasticity}$ are almost identical. In this example, computed with either 3- or 6-node triangular elements, the rate of convergence of the error in elasticity is almost the same because of the presence of singularities.

Thus, let us consider a problem where the elastic solution is perfectly regular. The finite element analysis is conducted on the beam in Figure 4(a) with a 70-element mesh (Figure 9), then with 3 other meshes obtained by successive refinements (see Table III).

Figure 10 shows once again a similar evolution for I^2_{space} and $e^2_{elasticity}$. More precisely, on the two finer meshes, we obtain

$$I_{space} = O(h^{1.6}) \quad \text{and} \quad e_{elasticity} = O(h^{1.9})$$

Again, the rates of convergence of the indicator in space I_{space} and the error in elasticity $e_{elasticity}$ are very similar, and their values are close to 2, the theoretical rate of convergence in elasticity for 6-node elements.

In conclusion, the previous examples have shown that it is reasonable to consider that the part of the error due to the spatial discretization evolves, relative to the size of the elements, much the same as the error in elasticity evolves.

Table II. Results for 6-node triangular elements

Number of elements	e^2	i^2_{time}	I^2_{space}	$e^2_{elasticity}$
92	76·81	7·89	68·92	0·2398
368	21·81	8·21	13·60	0·0518
1472	11·12	8·18	2·94	0·0128
5888	8·97	8·16	0·81	0·0034

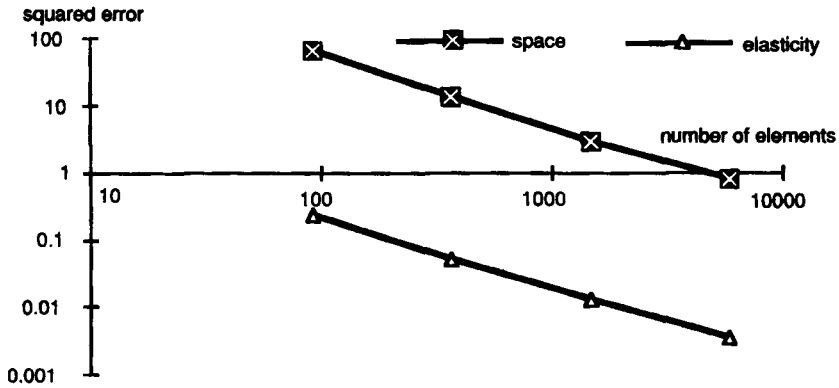

Figure 8. Evolution of I^2_{space} and $e^2_{elasticity}$ as a function of the number of elements

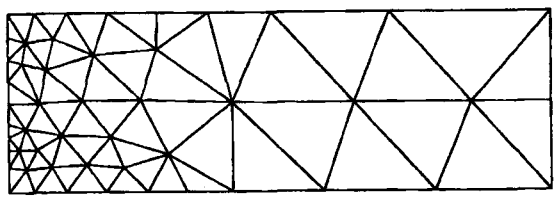

Figure 9. 70-element mesh

Table III. Results for 6-node triangular elements

Number of elements	e^2	i^2_{time}	e^2_{space}	$e^2_{elasticity}$
70	180·1	9·96	170·1	0·7709
280	34·80	10·43	24·38	0·0584
1120	13·84	10·46	3·41	0·0041
4480	10·76	10·339	0·37	0·00027

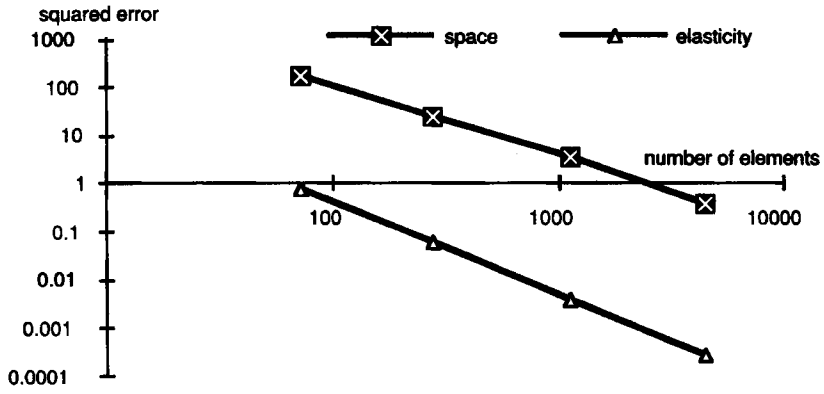

Figure 10. Evolution of I^2_{space} and $e^2_{elasticity}$ as a function of the number of elements

A simple procedure of adaptivity

This first procedure consists of using sufficiently fine time discretizations to be able to neglect the part of the error due to time in comparison with the part of the error due to space. This procedure may be described in the following way: Let ε_0 be the prescribed accuracy.

(1) An initial analysis over the time interval $[0, T]$ is performed on a mesh $\mathbf{T}_e$ (previously optimized in elasticity) for a time discretization Δ. Then, the global error ε and the indicator in time i_{time} are computed.

(2) If $i_{time} \leqslant \theta\varepsilon_0$, it is considered that the errors due to the time discretization may be neglected. And, the characteristics of the optimal mesh $\mathbf{T}^*$ are determined by using the procedure developed in elasticity (the main ideas of this procedure may be found in the Appendix).

(3) If $i_{time} > \theta\varepsilon_0$, a new time discretization Δ^* is determined, in the part of $[0, T]$ where the loading leads to plastic behaviour, with the aim of satisfying $i^*_{time} \leqslant \theta\varepsilon_0$. The size Δt^* of the time steps is computed using (36) with respect to the size Δt of the time steps of Δ:

$$\Delta t^* = \frac{\theta\varepsilon_0}{i_{time}} \Delta t \tag{39}$$

A subsequent analysis is performed with Δ^* on the initial mesh $\mathbf{T}_e$. In one step, this procedure generally leads to obtaining the desired inequality and the point (2) above is then applied.

In this procedure, the time error indicator must be small in comparison to the global error. Thus, $\theta\varepsilon_0$ must be small in comparison to ε_0. In practice, we use $\theta = \frac{1}{3}$. Two examples of this procedure follow.

First example: The example of the console described in Figure 6(a) is considered again. The prescribed accuracy is $\varepsilon_0 = 5$ per cent. The initial mesh used (Figure 11(a)) has 273 6-node triangular elements. The time discretization has time step for the elastic loading and 2 time steps for the plastic loading whose length is

$$\Delta t = 40$$

The errors computed are (Figure 11(b))

$$\varepsilon = 11{\cdot}7 \text{ per cent} \quad \text{and} \quad i_{time} = 6{\cdot}8 \text{ per cent}$$

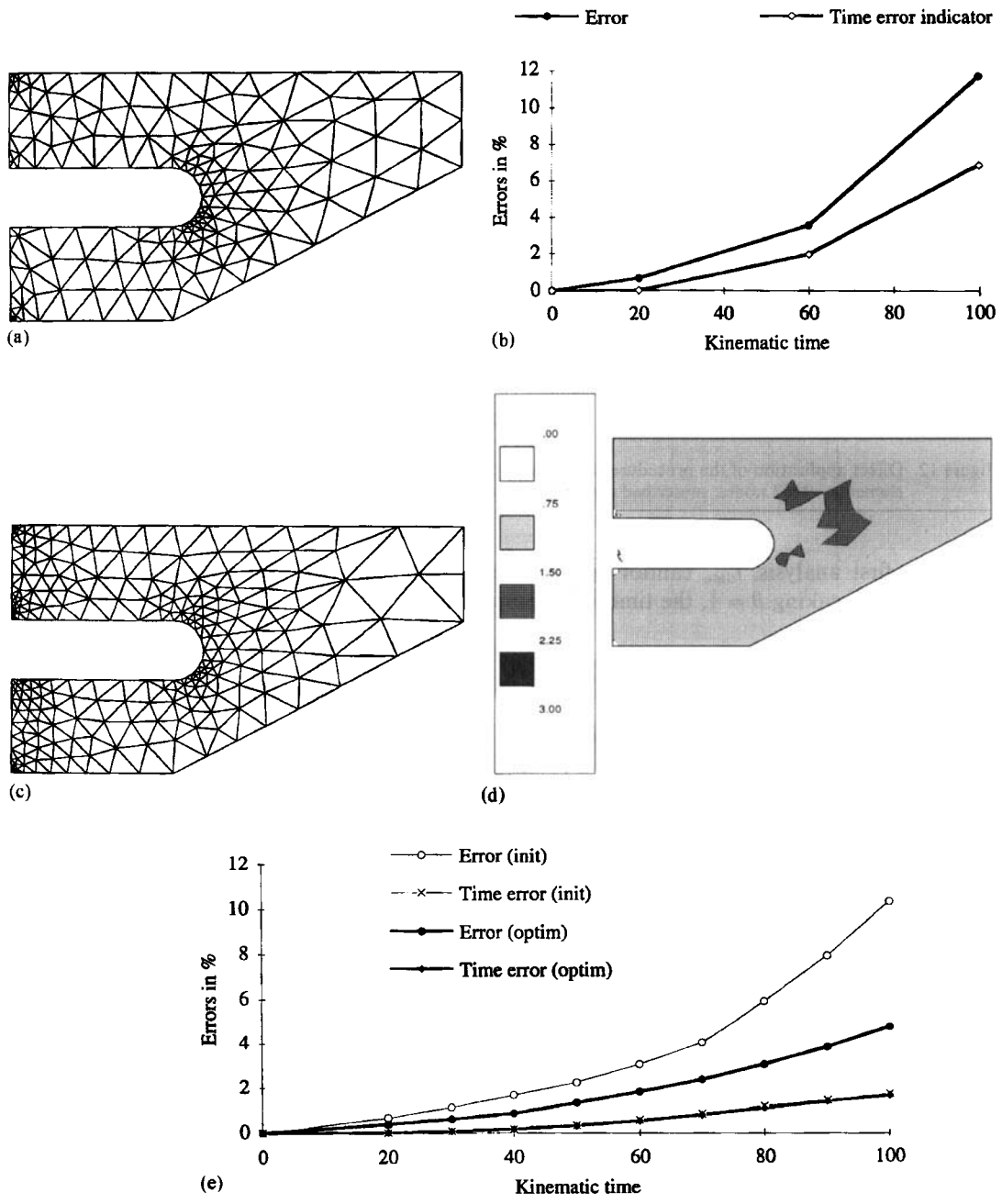

Figure 11. Adaptivity of the computation for the console; prescribed accuracy 5 per cent (a) Initial mesh, 273 6—node triangular elements—618 nodes, error 11·7 per cent (b) Contributions $\varepsilon_{[0,t]}$ and $i_{\text{time},[0,t]}$, 1 elastic increment, 2 plastic increments, $\Delta t = 40$ (c) Optimized mesh, 448 6-node triangular elements—999 nodes, error 4·7 per cent (d) Optimality map (e) Contributions $\varepsilon_{[0,t]}$ and $i_{\text{time},[0,t]}$; initial mesh and optimized mesh, 1 elastic increment, 8 plastic increments, $\Delta t = 10$

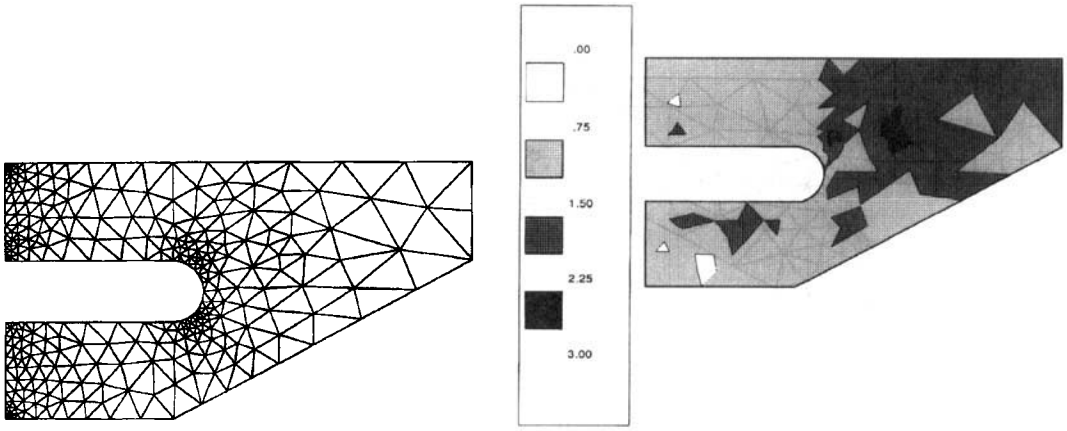

(a) (b)

Figure 12. Direct application of the procedure for an overly large time step (a) Optimized mesh, 530 6-node triangular elements—1167 nodes; prescribed accuracy: 5 per cent; obtained 8 per cent (b) Optimality map

In this first analysis, i_{time} cannot be neglected. So, a new time discretization is computed beforehand. In taking $\theta = \frac{1}{3}$, the time step computed is

$$\Delta t^* = 10$$

Using this new time discretization, the errors computed are (Figure 11(e))

$$\varepsilon = 10{\cdot}3 \text{ per cent} \quad \text{and} \quad I_{\text{time}} = 1{\cdot}68 \text{ per cent}$$

The inequality $i^*_{\text{time}} \leqslant \theta\varepsilon_0$ is then satisfied, and point (2) described above may be applied. The optimized mesh thus determined is shown in Figure 11(c), and the errors computed are (Figure 11(e))

$$\varepsilon^* = 4{\cdot}7 \text{ per cent} \quad \text{and} \quad i^*_{\text{time}} = 1{\cdot}61 \text{ per cent}$$

To control the optimality of the mesh, a simple method consists of determining a map of optimal sizes for a prescribed accuracy equal to the obtained accuracy ε^* (neglecting once again the errors due to the time discretization). If the built mesh is correctly optimized, the procedure must yield for each element a coefficient of modification of size r_E close to 1. In practice, a mesh is correctly optimized if, for the majority of the elements, $0{\cdot}75 \leqslant r_E \leqslant 1{\cdot}5$. Figure 11(d) shows that the mesh $\mathbf{T}^*$ is very well-optimized.

It must be noted that direct application of point (2) above, without having previously determined a new time discretization, leads to the mesh shown in Figure 12(a) and to an error of 8 per cent, compared with the prescribed 5 per cent. Besides, Figure 12(b) shows that this mesh is not optimal.

Second example: The example of the axisymmetric press described in Figure 3(a) is considered again. The prescribed accuracy is 2 per cent. The initial mesh is shown in Figure 13(a), and the

Figure 13. Adaptivity of the computation for the press; prescribed accuracy 2 per cent (a) Initial mesh, 211 6-node triangular elements—486 nodes, error 6·3 per cent (b) Optimized mesh, 677 6-node triangular elements—1466 nodes, error 2·3 per cent (c) Contributions $\varepsilon_{[0,t]}$ and $i_{\text{time},[0,t]}$; initial mesh and optimized mesh (d) Optimized mesh, optimality map (e) Regular mesh, 680 6-node triangular elements—1463 nodes, error 5·6 per cent

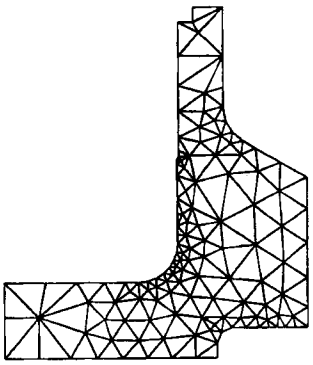

(a)

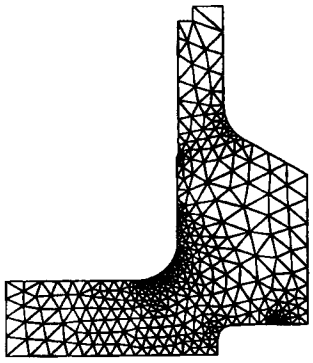

(b)

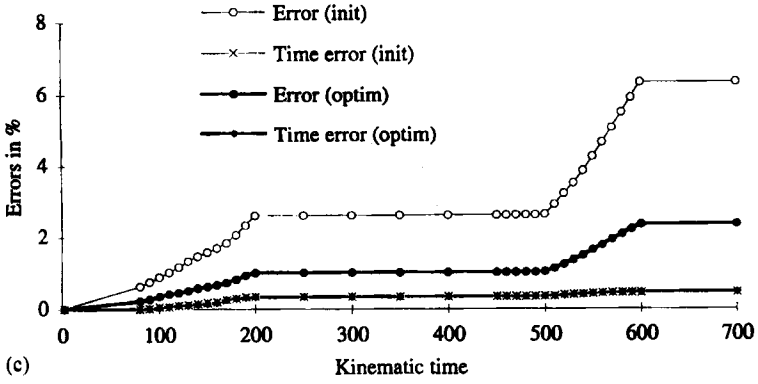
Error (init)
Time error (init)
Error (optim)
Time error (optim)
Errors in %
8
6
4
2
0
0
100
200
300
400
500
600
700
Kinematic time

(c)


.00
.75
1.50
2.25
3.00

(d)

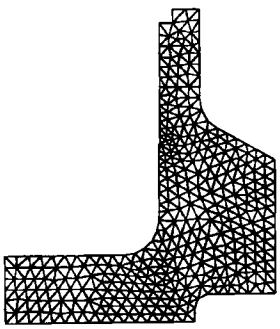

(e)

time discretization has 35 time steps. The errors computed are: $\varepsilon = 6{\cdot}3$ per cent and $i_{\text{time}} = 0{\cdot}43$ per cent. In applying the procedure the mesh $\mathbf{T}^*$ (Figure 13(b)) is obtained in one step, and the errors computed are $\varepsilon^* = 2{\cdot}3$ per cent and $i^*_{\text{time}} = 0{\cdot}44$ per cent.

Figure 13(c) shows the evolution of the contributions $\varepsilon_{[0,t]}$ and $i_{\text{time},[0,t]}$ on the initial mesh and on the optimized mesh, and Figure 13(d) allows controlling the optimality of the built mesh. In comparison, Figure 13(e) shows a regular mesh including almost the same number of nodes as the optimized mesh. The errors computed on this mesh are $\varepsilon = 5{\cdot}5$ per cent and $i_{\text{time}} = 0{\cdot}63$ per cent.

These examples show that this first procedure functions correctly. Yet, it is clear that the main drawback of this technique is that the possibilities of optimizing the time discretization are neglected.

Simultaneous adaptivity of the space–time parameters

The idea herein is to use more completely the decomposition $\mathbf{e}^2 = \mathbf{I}^2_{\text{space}} + \mathbf{I}^2_{\text{time}}$ introduced in (37). Let us recall that evaluating $\mathbf{I}_{\text{time}}$ with $\mathbf{i}_{\text{time}}$, we get the following evaluation for $\mathbf{I}_{\text{space}}$:

$$\mathbf{I}^2_{\text{space}} = \mathbf{e}^2 - \mathbf{i}^2_{\text{time}}$$

To determine a size map, the contributions of each element E of the mesh to $\mathbf{I}_{\text{space}}$ must be known. First of all, it seems logical to define these quantities by

$$\mathbf{I}^2_{\text{space},E} = \mathbf{e}^2_E - \mathbf{i}^2_{\text{time},E} \tag{40}$$

For the global error, in all the examples computed, we have always noted $\mathbf{e}^2 > \mathbf{i}^2_{\text{time}}$. However, for very fine meshes and coarse time discretizations, it may be observed on some elements that $\mathbf{e}^2_E \leqslant \mathbf{i}^2_{\text{time},E}$. To avoid this difficulty, we have chosen to define the local contributions of an element by

$$\mathbf{I}^2_{\text{space},E} = \text{Sup}\,[0, \mathbf{e}^2_E - \mathbf{i}^2_{\text{time},E}] \tag{41}$$

Hence

$$\mathbf{I}^2_{\text{time},E} = \mathbf{e}^2_E - \mathbf{I}^2_{\text{space},E} = \begin{cases} \mathbf{i}^2_{\text{time},E} & \text{if } \mathbf{I}^2_{\text{space},E} > 0 \\ \mathbf{e}^2_E & \text{otherwise} \end{cases} \tag{42}$$

And for the whole structure,

$$\mathbf{I}^2_{\text{space}} = \sum_E \mathbf{I}^2_{\text{space},E} \quad \text{and} \quad \mathbf{I}^2_{\text{time}} = \sum_E \mathbf{I}^2_{\text{time},E} \tag{43}$$

This allows obtaining (37) once again.

These quantities may be associated with relative ones:

$$\varepsilon = \frac{\mathbf{e}}{D}, \quad I_{\text{time}} = \frac{\mathbf{I}_{\text{time}}}{D}, \quad I_{\text{space}} = \frac{\mathbf{I}_{\text{space}}}{D} \tag{44}$$

where D is the denominator defined in (12).

For a prescribed global error of ε_0, the following procedure may be defined:

(1) An initial analysis over the time interval $[0, T]$ is performed on a mesh $\mathbf{T}_e$ (previously optimized in elasticity) for a time discretization Δ. Then, the global error ε, the time indicator I_{time} and the space indicator I_{space} are computed.

(2) A new mesh T^* and a new time discretization Δ^* are determined in order to equally split the optimized error between the space error and the time error:

$$\begin{cases} \varepsilon^* = \varepsilon_0 \\ I^*_{\text{time}} = I^*_{\text{space}} \end{cases} \tag{45}$$

The time discretization Δ^* is computed such that $I^{*2}_{\text{time}} = \frac{1}{2}\varepsilon_0^2$. In order to obtain during the optimized computation $I^*_{\text{time}} = I^*_{\text{space}}$. Thus, the length of the time step is determined uniformly by

$$\Delta t^* = \frac{1}{\sqrt{2}} \frac{\varepsilon_0}{I_{\text{time}}} \Delta t \tag{46}$$

Obviously, this modification of the size of the time step is not performed on the first elastic increment.

The mesh $\mathbf{T}^*$ is built using the techniques developed in statics for a prescribed spatial error: $I^*_{\text{space}} = \frac{1}{2}\varepsilon_0^2$.

Remark. To represent correctly the loading history, it may be necessary to fix a limit $\Delta t_{\max}$ for the length Δt^* of each time step. If this maximum length is reached during the computation of Δ^*, Δt^* is chosen equal to $\Delta t_{\max}$, and it is no more possible to equally split the optimized error between the space error and the time error. Equations (36) and (37) lead us to built the optimized mesh $\mathbf{T}^*$ for a prescribed spatial error:

$$I^*_{\text{space}} = (1 - \alpha)\,\varepsilon_0^2 \quad \text{where} \quad \alpha = \frac{\Delta t_{\max}}{\Delta t} \frac{I_{\text{time}}}{\varepsilon_0}$$

To illustrate this procedure, we re-examine the example of the console (Figure 6(a)). The initial analysis is conducted with a 273-element mesh (Figure 14(a)) and a coarse time discretization (1 time step of elastic loading and 2 time steps of plastic loading). The prescribed error is 5 per cent.

The initial analysis leads to $\varepsilon = 11{\cdot}7$ per cent and $i_{\text{time}} = 6{\cdot}8$ per cent. The simultaneous adaptivity procedure leads to the use of a 5-increment time discretization with a 621-element optimized mesh, as shown in Figure 14(b). The errors computed are then $\varepsilon^* = 5{\cdot}0$ per cent and $i^*_{\text{time}} = 3{\cdot}3$ per cent.

Figure 14(c) shows the evolution of the contributions $\varepsilon_{[0,t]}$ and $i_{\text{time},[0,t]}$ on the initial mesh and on the optimized mesh. In this example, the simultaneous procedure leads to a reduction of the computer processing time of roughly 25 per cent (see Table IV).

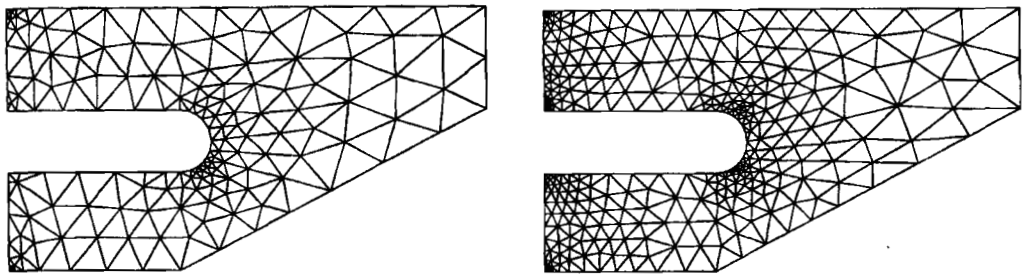

(a) (b)

Figure 14 (a–b)

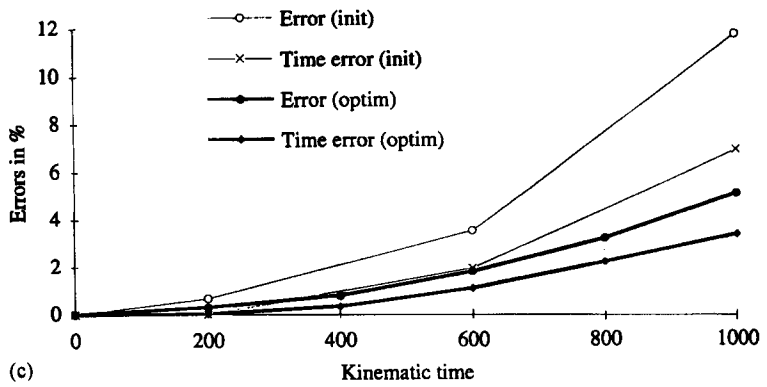

Figure 14. Simultaneous adaptivity in time and space for the computation of the console; prescribed accuracy 5 per cent (a) Initial mesh, 273 6-node triangular elements—618 nodes, error 11·7 per cent (b) Optimized mesh, 621 6-node triangular elements—1366 nodes, error 5·0 per cent. (c) Contributions $\varepsilon_{[0,t]}$ and $i_{temps,[0,t]}$, initial mesh: 1 elastic increment, 2 plastic increments; optimized mesh: 1 elastic increment, 4 plastic increments

Table IV. Comparison between the efficiencies of the two procedures

Procedure	Simple	Simultaneous
Number of elements	448	621
Number of nodes	99	1366
Number of increments	9	5
Computed error	4·7 per cent	5·0 per cent
Computer processing time (HP 735)	115 s	90 s

CONCLUSION

An error measure with a strong mechanical meaning has been implemented to control the finite element analysis in elastoplasticity. This error measure enables taking into account all the errors due to the discretization: errors due to the spatial discretization, errors due to the incremental method. Initially, it has been implemented for the Prandtl–Reuss constitutive relation in elastoplasticity for 2-D or axisymmetric problems and for 3- or 6-node triangular elements. It must be noted that this implementation is independent from the algorithm used to solve the plasticity problem.

The extension of this error measure to other constitutive relations in elastoplasticity does not present any difficulties, under the condition that these relations strictly satisfy Drucker's inequality. In the same way, the extension to quadrilaterals and even to tetrahedrons may be easily implemented by using the techniques of construction of admissible fields proposed in Ladevèze *et al.*[24,30]

The time error indicator that we have built allows separating the contribution to the error due to the spatial discretization from the contribution due to the incremental method. Using these contributions and their spatial distributions, two procedures of adaptivity of the computation parameters have been proposed. The first one imposes the use of sufficiently fine time discretization to that the associated contribution is negligible in comparison with the error due to the spatial discretization. In this case, the adaptivity of the computation is confined to the adaptivity

of the mesh. The second one is an initial example of a procedure allowing to simultaneously adapt the mesh and the length of the time increments. The example presented shows that this procedure leads to a significant reduction in computation cost. The very simple strategy employed that consists of balancing the contributions in space in time, is independent of the algorithm used. Nevertheless, for a prescribed accuracy, this strategy does not necessarily lead to the lowest computation cost. A better optimization of the computation cost would require taking into account the algorithm used.

APPENDIX

Construction of $\sigma_{SA}(t_{i+1})$ *from* $\sigma_h(t_{i+1})$

To perform the construction, we impose $\sigma_{SA}(t_{i+1})$ to be linked to $\sigma_h(t_{i+1})$ by the following conditions:

$$\int_E (\sigma_{SA}(t_{i+1}) - \sigma_h(t_{i+1}))^T \varepsilon(\varphi_i)\, dE = 0 \tag{47}$$

which must be satisfied for all functions of basis φ_i associated with the finite element discretization and for each element E of the mesh.

In a first step, in using (2b) and (47), we determine on the faces of the elements, from local node-by-node computations, the densities of forces $\hat{F}(t_{i+1})$ such that

$$\int_E f_d(t_{i+1})^T U^* dE + \int_{\partial_2 E} \eta_E \hat{F}(t_{i+1})^T U^* dS = 0 \tag{48}$$

for all U^*, solid displacement field on the element E. In (48), $\eta_E = \pm 1$ and is constant on each edge of E. Moreover, on an edge common to two elements E_1 and E_2, we have

$$\eta_{E_1} + \eta_{E_2} = 0 \tag{49}$$

In a second step, the stress field $\sigma_{SA}(t_{i+1})$ is built on each element E in determining a simple solution of the equilibrium equations:

$$\begin{aligned} &\operatorname{div} \sigma_{SA}(t_{i+1}) + f_d(t_{i+1}) = 0 \quad \text{in } E \\ &\sigma_{SA}(t_{i+1}) n = \eta_E \hat{F}(t_{i+1}) \quad \text{on } \partial E \end{aligned} \tag{50}$$

(where n denotes, on ∂E, the unitary normal outside vector). Indeed, the condition (48) shows that (50) admits solutions. We must note that (48) is still satisfied when on an edge Γ, the density $\hat{F}(t_{i+1})$ built is replaced by $\hat{F}(t_{i+1}) + \hat{H}$, where $\hat{H}$ denotes the density of forces with a zero resultant and moment on Γ.

As an example, for the 3-node triangular elements, $\hat{F}(t_{i+1})$ is built in a linear fashion on each edge Γ:

$$\hat{F}(t_{i+1}) = A + (\lambda_1 - \lambda_2) B \tag{51}$$

with A and B constant vectors, and λ_1 and λ_2 barycentric co-ordinates on the edge Γ. In taking

$$\hat{H} = (B^T \mathbf{t})(\lambda_2 - \lambda_1)\mathbf{t} \tag{52}$$

where $\mathbf{t}$ denotes a unitary vector tangent to Γ, we obtain fields $\sigma_{SA}(t_{i+1})$ that lead to an error measure of better quality.

Optimal mesh

In elasticity, we use the criterion of optimality introduced by Ladevèze *et al.*;[4] a mesh $\mathbf{T}^*$ is optimal relative to a measure of error ε if

$$\begin{aligned} &\varepsilon^* = \varepsilon_0 \text{ prescribed accuracy} \\ &N^* \text{ minimal number of elements} \end{aligned} \tag{53}$$

This criterion of optimality naturally leads to minimizing the costs of computations. To solve the problem (53), the following procedure is used:

An initial analysis is performed on a relatively coarse mesh $\mathbf{T}$.
For this mesh, the global error ε and the local contributions ε_E are computed.
The characteristics of the optimal mesh $\mathbf{T}^*$ are determined.

Then, the mesh $\mathbf{T}^*$ is generated by an automatic mesh generator and a second finite element computation is made.

To determine the characteristics of the optimal mesh $\mathbf{T}^*$, the method consists of computing on each element E of the mesh $\mathbf{T}$ a coefficient of size modification:

$$r_E = \frac{h_E^*}{h_E} \tag{54}$$

where h_E denotes the size of the element E and h_E^* the size to be imposed to the elements of $\mathbf{T}^*$ in the region of E to assure the optimality. The computation of the coefficients r_E is based on the rate of convergence of the error:

$$\varepsilon = O(h^q) \tag{55}$$

where q depends upon the type of element used, but equally upon the regularity of the solution.

Let us suppose that the solution of the problem is regular. Then, q is equal to the convergence rate of the used element. For instance, we have $q = 1$ for the 3-node triangular elements and $q = 2$ for the 6-node triangular elements. In this case, to predict the optimal sizes we write that the ratio of the sizes is linked to the ratio of the errors by

$$\frac{\varepsilon_E^*}{\varepsilon_E} = \left[\frac{h_E^*}{h_E}\right]^q = r_E^q \tag{56}$$

where ε_E^* denotes the contribution of the elements of $\mathbf{T}^*$ situated in the area E.

The square of the error on the mesh $\mathbf{T}^*$ can be evaluated by

$$\sum_E (\varepsilon_E^*)^2 = \sum_E r_E^{2q}\, \varepsilon_E^2 \tag{57}$$

and the number of elements of $\mathbf{T}^*$ by

$$N^* = \sum_E \frac{1}{r_E^2} \tag{58}$$

The problem (53) thereby becomes

$$\text{Minimize } N^* = \sum_E \frac{1}{r_E^2} \quad \text{with} \quad \sum_E r_E^{2q}\, \varepsilon_E^2 = \varepsilon_0^2 \tag{59}$$

whose explicit solution is given by

$$r_E = \frac{\varepsilon_0^{1/q}}{\varepsilon_E^{1/(q+1)} \left[\sum_E \varepsilon_E^{2/(q+1)}\right]^{1/2q}} \tag{60}$$

REFERENCES

1. P. Ladevèze and D. Leguillon, 'Error estimate procedure in the finite element method and applications', *SIAM J. Numer. Anal.*, **20**, no 3, 485–509 (1983).
2. D. W. Kelly, J. P. Gago, O. C. Zienkiewicz and I. Babuska, '*A posteriori* error analysis and adaptive processes in the finite element method: Part I—error analysis', *Int. j. numer. methods eng.*, **19**, 1593–1619 (1983).
3. J. P. Gago, D. W. Kelly, O. C. Zienkiewicz and I. Babuska, '*A posteriori* error analysis and adaptive processes in the finite element method: Part II—adaptive mesh refinement', *Int. j. numer. methods eng.*, **19**, 1621–1656 (1983).
4. P. Ladevèze, G. Coffignal and J. P. Pelle, 'Accuracy of elastoplastic and dynamic analysis', in I. Babuska, O. C. Zienkiewicz, J. P. Gago and A. E. Oliveira (eds.), *Accuracy Estimates and Adaptivity for Finite Elements*, Wiley, New York, 1986, Chapter 10, pp. 181–203.
5. O. C. Zienkiewicz and J. Z. Zhu, 'A simple error estimator and adaptive procedure for practical engineering analysis', *Int. j. numer. methods eng.*, **24**, 337–357 (1987).
6. J. T. Oden, L. Demkowicz, W. Rachowicz and T. A. Westermann, 'Toward a universal h–p adaptive finite element strategy: part 2—*a posteriori* error estimation', *Comput. Methods Appl. Mech. Eng.*, **77**, 113–180 (1989).
7. T. Strouboulis and K. Haque, 'Recent experiences with error estimator and adaptivity, Part I: review of error estimators for scalar elliptic problems', *Comput. Methods Appl. Mech. Eng.*, **97**, 113–180 (1989).
8. G. Coffignal and P. Ladevèze, 'Error computation and optimal mesh in elasticity and elastoplasticity', *Proc. SMIRT 7*, North-Holland, Amsterdam, 1983, Vol. L. pp. 177–182.
9. W. K. Liu, T. Belytschko and H. Chang, 'An arbitrary Lagrangian–Eulerian finite element method for path-dependent materials', *Comput. Methods Appl. Mech. Eng.*, **58**, 227–245 (1986).
10. J. T. Oden, T. Strouboulis and P. Devloo, 'Adaptive finite element methods for the analysis of inviscid compressible flow: Part I. Fast refinement/unrefinement and moving mesh methods for unstructured meshes', *Comput. Methods Appl. Mech. Eng.*, **59**, 327–362 (1986).
11. O. C. Zienkiewicz, Y. C. Liu and G. C. Huang, 'Error estimation and adaptivity in flow formulation for forming problems', *Int. j. numer. methods eng.*, **25**, 23–42 (1988).
12. H. Jin, L. Bernspang, R. Larsson and N. E. Wiberg, 'Mesh generation and mesh refinement procedures for computational plasticity', *Proc. Int. Conf. Comp. Plas.*, Barcelone, 1990, pp. 347–358.
13. C. Bajer, R. Bogacz and C. Bonthoux, 'Adaptive space–time elements in dynamic elastic–viscoplastic problem', *Comput. Struct.*, **39**, 415–423 (1991).
14. C. Johnson and P. Hansbo, 'Adaptive finite element methods for small strain elasto-plasticity', *Proc. IUTAM Conf. on Finite Inelastic Deformations–Theory and Applications*, University of Hannover, 1991, pp. 273–288.
15. M. Ortiz and J. J. Quigley, 'Adaptive mesh refinement in strain localization problems', *Comput. Methods Appl. Mech. Eng.*, **90**, 781–804 (1991).
16. D. Aubry and B. Tie,'*A posteriori* error analysis and h adaptive refinement for the FEM in non linear structural computations', *Proc. European Conf. on New Advances in Computational Structural Mechanics*, Giens, 1991, pp. 1–8.
17. W. Rust and E. Stein, '2D-finite-element mesh adaptations in structural mechanic, including shell analysis and non-linear calculations', in P. Ladevèze and O. C. Zienkiewicz (eds.), *New Advances in Computational Structural Mechanics*, Elsevier, Amsterdam, 1992, pp. 219–232.
18. K. Kato, N. S. Lee and K. J. Bathe, 'Adaptive finite element analysis of large strain elastic response', *Comput. Struct.*, **47**, 829–855 (1993).
19. D. R. J. Owen, D. Peric and J. Yu, 'On error estimate and adaptivity in elasto-plastic solids', *Int. j. numer. methods eng.*, to be published.
20. P. Ladevèze, 'Sur une famille d'algorithmes en Mécanique des Structures', *C. R. Acad. Sci. Paris* (t 300, série II), **2**, 41–44 (1985).
21. D. C. Drucker, 'On the postulate of stability of materials in the mechanics of continua', *J. de Mècanique*, **3**, 235–245 (1964).
22. D. R. J. Owen and E. Hinton, *Finite Elements in Plasticity*, 2nd edn, Pineridge, Swansea, 1986.
23. K. J. Bathe, *Finite Element Procedures in Engineering Analysis*, Prentice-Hall, Englewood Cliffs, N.J., 1982.
24. P. Ladevèze and J. P. Pelle and P. Rougeot, 'Error estimation and mesh optimization for classical finite elements', *Eng. Comp.*, **8**, 69–80 (1991).
25. P. Coorevits, P. Ladevèze and J. P. Pelle, 'An automatic procedure for finite element analysis in 2D elasticity with a control of accuracy', *Comput. Methods Appl. Mech. Eng.*, **121**, 91–120 (1995).
26. M. Ortiz and J. C. Simo, 'An analysis of a new class of integration algorithm for elastoplastic constitutive relations', *Int. j. numer. methods eng.*, **23**, 353–366 (1985).
27. P. Jetteur, 'Implicit integration algorithm for elastoplasticity in plane stress analysis', *Eng. Comp.*, **3**, 251–253 (1986).
28. P. Gratacos, P. Montmitonnet and J. L. Chenot, 'An integration scheme for Prandtl–Reuss elasto-plastic constitutives equations', *Int. j. numer. methods eng.*, **33**, 943–961 (1992).
29. P. Verpeaux, T. Charass and A. Millard, 'CASTEM 2000: une approche moderne du calcul des structures', in J. M. Fouet, P. Ladevèze and R. Ohayon (eds.), *Calcul des Structures et Intelligence Artificielle*, Pluralis, 1988, Vol. 2, pp. 261–271.
30. J. L. Gastine, P. Ladevèze, P. Marin and J. P. Pelle, 'Accuracy and optimal meshes in finite element computation for nearly incompressible materials', *Comput. Methods Appl. Mech. Eng.*, **94**, 303–315 (1992).